Catal Lett
DOI 10.1007/s10562-015-1492-9

Synthesis and Heterogenization of Siloxane Functionalized Cobalt Complex: Potential Catalyst for Oxidation of Alcohols

**T. Baskaran · R. Kumaravel · J. Christopher ·
S. Radhakrishnan · A. Sakthivel**

Received: 17 December 2014 / Accepted: 30 January 2015

Abstract Cobalticinium complex containing siloxane moiety on ligand center was first time synthesized, characterized and heterogenized on the surface of SBA-15 molecular sieves. FT-IR and ^{29}Si-MAS-NMR spectrum evidence the successful grafting of the cobalt complex on the surface of SBA-15. N_2 sorption isotherm of cobalticinium complex grafted sample showed the decrease in surface area, pore volume, further confirms the presence of complex inside the channel of mesoporous SBA-15. The heterogenized complex exhibited promising activity for oxidation of alcohols with good selectivity of ketone. Further the catalytic activity remains intact after two recycles.

Graphical Abstract Cobalticinium complex possessing siloxane functionality was prepared first time and heterogenized on SBA-15 surface. The resultant materials showed as promising recyclable heterogeneous catalyst for oxidation of alcohols.

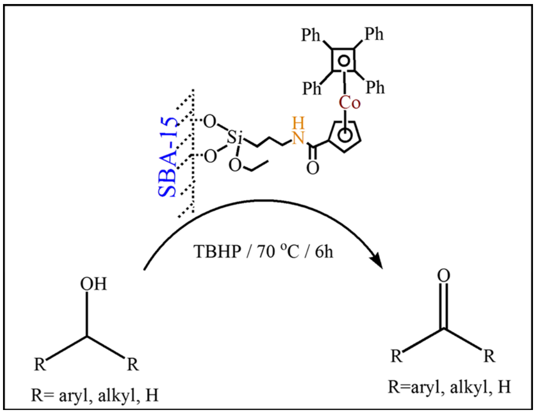

Keywords Cobalticinium complex · SBA-15 · Oxidation · Alcohols · Siloxane function

1 Introduction

In recent years, organometallic complexes containing siloxane functionality have great interest owing to their usefulness to bind covalently with hydroxyl group available on supported materials [1–6]. Several reports describing the molybdenum complexes with siloxane functionality present either in ligand center or metal centre, which were further heterogenized on the surface of silica has shown promising catalysts for various oxidation reactions [6–13]. Similarly, siloxane functionalized ruthenium and rhenium complexes are heterogenized on mesoporous molecular sieve surface has been applied for cyclo-propanation and epoxidation respectively [14, 15]. However, syntheses of first row transition metal complexes containing siloxane functional group are rare [3–5]. In addition, it

---

Electronic supplementary material The online version of this article (doi:10.1007/s10562-015-1492-9) contains supplementary material, which is available to authorized users.

T. Baskaran · R. Kumaravel · A. Sakthivel (✉)
Department of Chemistry, Inorganic Materials and Catalysis Laboratory, University of Delhi, New Delhi, India
e-mail: sakthiveldu@gmail.com; asakthivel@chemistry.du.ac.in

J. Christopher
R&D Centre, Indian Oil Corporation Ltd, Faridabad 121007, India

S. Radhakrishnan
NMR Lab, CSIR-Central Electrochemical Research Institute, Karaikudi 630 006, India

is well known that these metal complexes are potential substitution for expensive rare earth and late transition metal catalysts. Heterogenization of various transition metal based homogenous catalysis with salen, acac, and cyclopentadienyl-based ligands are shown very good catalytic ability for several oxidation reactions [16–21]. In this regard, cobalt based catalysts also shown comparable activity towards various organic transformations, such as hydroformylation, hydrosilylation, Fisher–Tropsch synthesis, hydroxylation, reforming, and various redox processes [22–31]. For example, cobalt-polyaniline nanostructure hosted SBA-15 shown as a capable catalyst for oxidation process [29]. Similarly, cobalt(II) complex grafted on SBA-15 has catalytic ability for acetylation of aldehydes and oxidation of alcohols at elevated temperature and microwave conditions using excess H_2O_2 [30, 31]. To the best of our knowledge, the structural stability and direct grafting of siloxane functionalized cobalt based complexes are not known. In this regard, it is worth mentioning here that the cobalticinium complexes are analogues to isoelectronic ferrocene complexes which has strong resistance under severe reaction conditions [32, 33]. It is interesting to develop stable full sandwich type complex, where the metal ion strongly hold with ligand and retain their active coordination sphere. It is well established that the cobalt based full sandwich complexes are highly stable and will be interesting to introduce siloxane functionality on these types of complexes. In an effort, herewith, we report the synthesis of siloxane functionalized cobalticinium complexes and heterogenized on SBA-15 molecular sieves. The resultant host–guest material is applied for liquid phase oxidation of alcohol at ambient reaction conditions.

2 Experimental Section

2.1 Solvents and General Procedures

All work up was carried out using standard Schlenk techniques under nitrogen atmosphere. THF and toluene were freshly distilled in-presence of sodium benzophenone; hexane was distilled over KOH and dichloromethane over calcium hydride under nitrogen atmosphere. ^{1}H, ^{13}C, NMR spectra were obtained using 400-MHz JEOL spectrometer.

2.2 Synthesis of (η^5-N-[3-(Triethoxysilyl) propylcarboxymidecyclopentadienyl) (η^4-tetraphenylcyclobutadiene)cobalt

Chlorotris(triphenylphosphine)cobalt and sodium carbomethoxycyclopentadienide (**2**) were prepared as per the procedure described in literature [34–36]. About 2.42 g (72 %) of the dried ligand **2**, was obtained. ^{1}H NMR (δ, 400 MHz, $CDCl_3$): 3.41(s, 3H, CH_3), 5.46 (t, 2H, Cp), 6.0 (t, 2H, Cp).

Freshly prepared chlorotris(triphenylphosphine)cobalt (7.24 g, 8.2 mmol) was added into the solution containing diphenyl acetylene (3.36 g, 18.9 mmol) dissolved in toluene (56 ml). The resultant solution was transferred to the flask containing sodium carbomethoxycyclopentadienide (**2**) (1.38 g, 9.4 mmol) in THF (14 ml). The final mixture was refluxed for 5 h and allowed to cool at room temperature. The solvent was removed under vacuum and the resultant residue was suspended in petroleum ether (50 ml) and collected by filtration to give compound **3**, as a yellow crystalline solid (4.06 g, 92 %): mp:222 °C; ^{1}H-NMR (400 MHz, $CDCl_3$) 3.14 (3 H, s, $–CH_3$) 4.7 (2 H, brs, CpH), 5.12 (2 H, brs, CpH) 7.15–7.22 (12 H, m, m and p-PhH) 7.37–7.34 (8 H, m, o-PhH):^{13}C (400 MHZ, $CDCl_3$) 51.6 ($–CH_3$), 76.4 (C_4Ph_4), 84.9 (CpC), 86.8 (CpC), 87.1 (ipso CpC), 127.1(p-PhC), 128.3(PhC), 129.2 (PhC), 135.5 (ipso-PhC), 167.0 ($–CO_2CH_3$).

Ester functional group of compound **3**, was hydrolysis using ethanolic potassium hydroxide solution to give rise to the corresponding acid (**4**) [34]. The resultant acid was extracted in ether (3 times, 30 ml) and dried. About 0.6 g (1.14 mmol) of acid, **4** was dissolved in CH_2Cl_2 (20 ml). The oxalyl chloride (0.1 ml, 1.4 mmol) was added to the above acid solution and the resulting red solution was stirred at room temperature for 30 min. The excess solvent and oxalyl chloride were removed under vacuum. The obtained crude acid chloride (**5**) was dissolved in CH_2Cl_2 (30 ml) and transferred to a flask containing the solution of N-(3-Triethoxysilyl) propyl amine (0.24 g, 1.14 mmol) in triethylamine (0.2 ml) and CH_2Cl_2 (6 ml). The resulting orange reaction mixture was stirred at room temperature for overnight and quenched with water (10 ml). The resultant complex was extracted with ethyl acetate (EtOAc; 30 ml). The organic phases were dried using anhydrous $MgSO_4$ and evaporated under vacuum to get the required product (**6**) of yellowish brown viscous oil. The schematic representation of preparation of complex **6** is shown in Scheme 1. The ^{1}H NMR spectrum is displayed in Fig. S1†, which evidences the formation of complex **6**. ^{1}H NMR (400 MHz, $CDCl_3$) 0.50–0.54 (t, 2 H, Si–CH_2), 1.20-1.27 (q, 9 H, CH_3), 1.38–1.40 (q, 2H, $CH_2–CH_2–CH_3$), 2.82–2.84 (q, 2 H, NCH_2), 3.78–3.82 (q, 6 H, O–CH_2–CH_3), 4.67 (s, 2H, CpH), 5.02 (s, 2H, CpH), 5.17 (s, 1 H, NH), 7.21–7.24 (12 H, m, *m*- and *p*- PhH), 7.43–7.47 (8 H, m, *o*-PhH) ^{13}C NMR(400 MHz, $CDCl_3$) 7.7 (Si–CH_2), 18.2 (CH_3), 23.1 (CH_2–CH_2-CH_2), 41.7 (NCH_2), 58.3 (CH_3-CH_2-O), 77.2 (C_4 Ph_4), 89.1 (CpC), 92.9 (ipso-CpC), 127.7 (p-PhC), 128.8 (PhC), 129.0 (PhC), 135.0 (ipso-PhC).

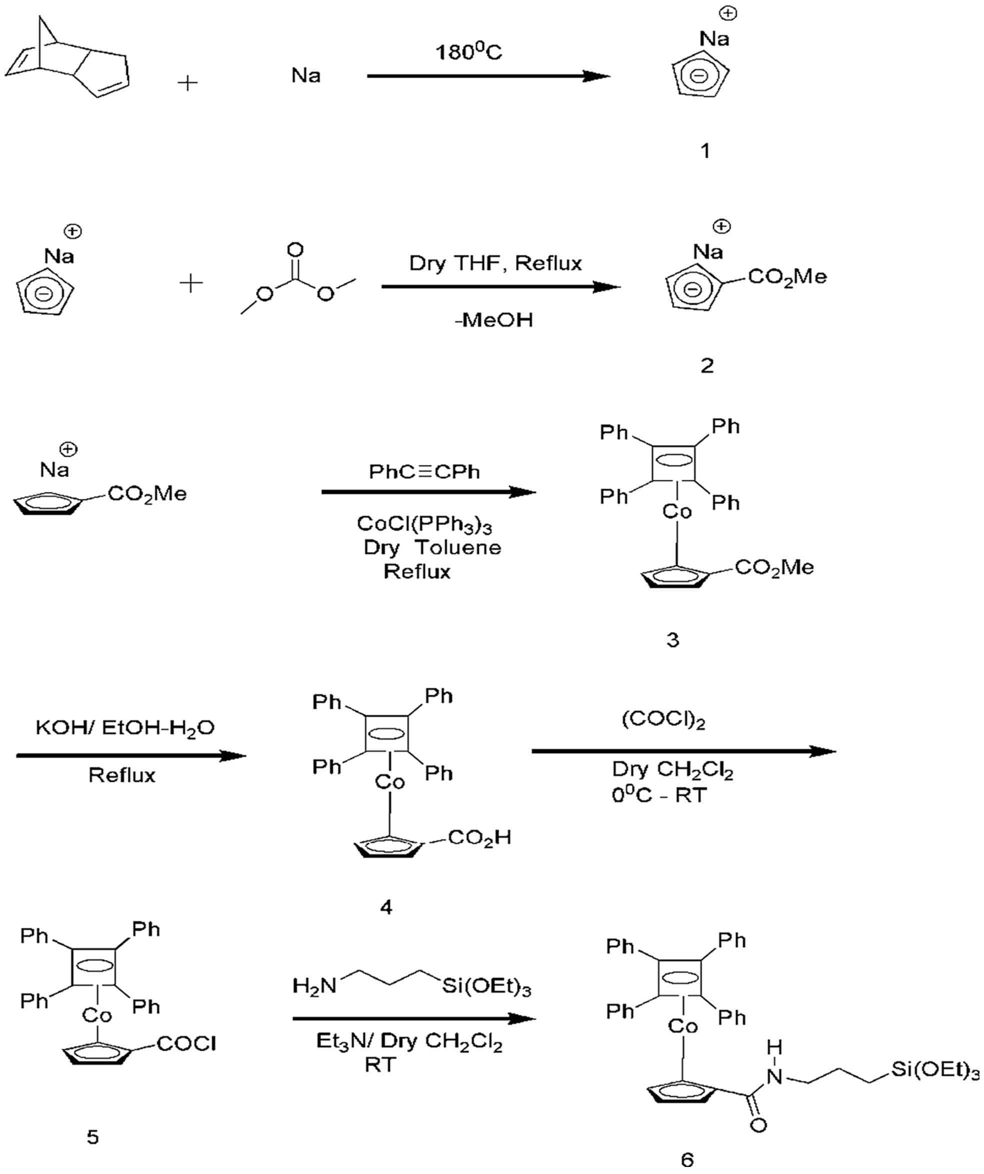

Scheme 1 Synthesis of complex (**6**)

2.3 Synthesis of Mesoporous SBA-15 and Heterogenization of Complex 6 on SBA-15

Mesoporous silica were synthesized as per the procedure described earlier [10–12] using pluronic 123 triblock copolymers (poly(ethylene oxide)-poly(propylene oxide)-poly(ethylene oxide); (Aldrich)) $EO_nPO_{70}EO_n$ as templates with the molar gel composition of the synthesis mixture was 6.89×10^{-4} P123 triblock copolymers : 0.24 HCl: 0.041 TEOS: 7.88 H_2O. The as-synthesized sample was calcined at 550 °C for 6 h in an atmospheric air.

The complex **6** was heterogenized on calcined SBA-15 molecular sieve as per the following procedure. First, a SBA-15 molecular sieve was pre-activated at 150 °C for overnight under vacuum in a Schlenk round bottom flask, and then it was cooled to room temperature under dry nitrogen atmosphere. About 1 mmol of complex **6** in toluene (30 ml) was introduced to 1 gm of pre-activated SBA-15 molecular sieves. The mixture was refluxed for 6 h, and then the solvent was removed under vacuum, washed with dichloromethane and dried under vacuum. The heterogenized cobalticinium complex (**6**) on SBA-15 was designated as SBA-15Co–Si.

2.4 Characterization of Materials

The crystallinity of the grafted materials was studied by powder XRD using a 18 KW Rigaku (2,500 V), Japan with Cu-Kα radiation ($\lambda = 1.54184$ Å). The diffraction patterns were recorded in the 2θ range of 0.5–10°, with a scan speed and step size of 1° per minute and 0.02°, respectively. FT-IR spectra were obtained in the range 400–4,000 cm^{-1}

using KBr pellets (BRUKER, TENSOR 27 FT-IR Spectrometer). The textural properties (BET surface area, BJH pore volume) of the parent and grafted materials were derived from N_2 sorption analysis, which was carried out at −196 °C using an automatic micropore physisorption analyzer (Micromeritics ASAP 2020, USA) after the samples were degassed at 150 °C for at least 8 h under 10^{-3} Torr pressure prior to each run. Proton and carbon NMR spectra of complex were recorded on a JEOL AL-400 FT NMR instrument using $CDCl_3$ as solvent. The amount of cobalt loaded on SBA-15 was estimated by atomic absorption spectrophotometer (AAS, Analytic Jena; ZEEnit700 P) as per the procedure described below. First, about 100 mg of catalyst was digested with $HCl:HNO_3$ mixture (3:1), then the resultant solution filtered using whatman filter paper and made up to 100 ml using double distilled deionized water. Analysis was carried out using an air-acetylene flame at wavelength of 240.7 nm wavelength. The calibration curve was obtained using $Co(NO_3)_2{\cdot}6H_2O$ as standard at different concentration. The electronic spectra of grafted materials was studied using diffuse reflectance ultraviolet–visible (DRUV–Vis; UV-260Shimadzu) spectrometer. Solid-state NMR experiments were carried out on a Bruker AVANCE 400 narrow bore spectrometer equipped with a superconducting magnet with a field of 9.4 T using a 4 mm double resonance cross-polarized magic angle spinning (CP-MAS) probe operating at resonating frequencies of 79.4 and 100.6 MHz for ^{29}Si and ^{13}C respectively. The samples were packed in 4 mm zirconia rotors and subjected to a spinning speed of 5 kHz: single pulse experiment with pulse duration of 4 µs and a relaxation delay time of 5 s were used for recording ^{29}Si and ^{13}C MAS NMR pattern with 2000 number of scans. The chemical shift values are expressed with respect to TMS for the ^{29}Si and glycine ^{13}C nucleus. Thermogravimetry-analysis (TGA) was carried out using Thermal Analyzer (Model-2950, TA Instruments, and USA). About 5–10 mg of the sample was taken in the platinum pan under air atmosphere at the heating rate of 10 °C min^{-1} up to 800 °C.

2.5 Catalytic Oxidation of Alcohol Using SBA-15Co–Si

The catalytic activity was studied for oxidation of benzhydrol and other alcohols in liquid phase medium using TBHP in decane as oxidant (Scheme 2). After the reaction, catalyst was separated, washed with dichloromethane, dried in vacuum and reused. The product was collected and were analyzed using gas chromatography equipped with FID (Agilent 7890A Series) connected to a HP-5 capillary column (30 m; HP-5). The catalytic activity of pure SBA-15 and complex **6** were studied under identical conditions for comparison.

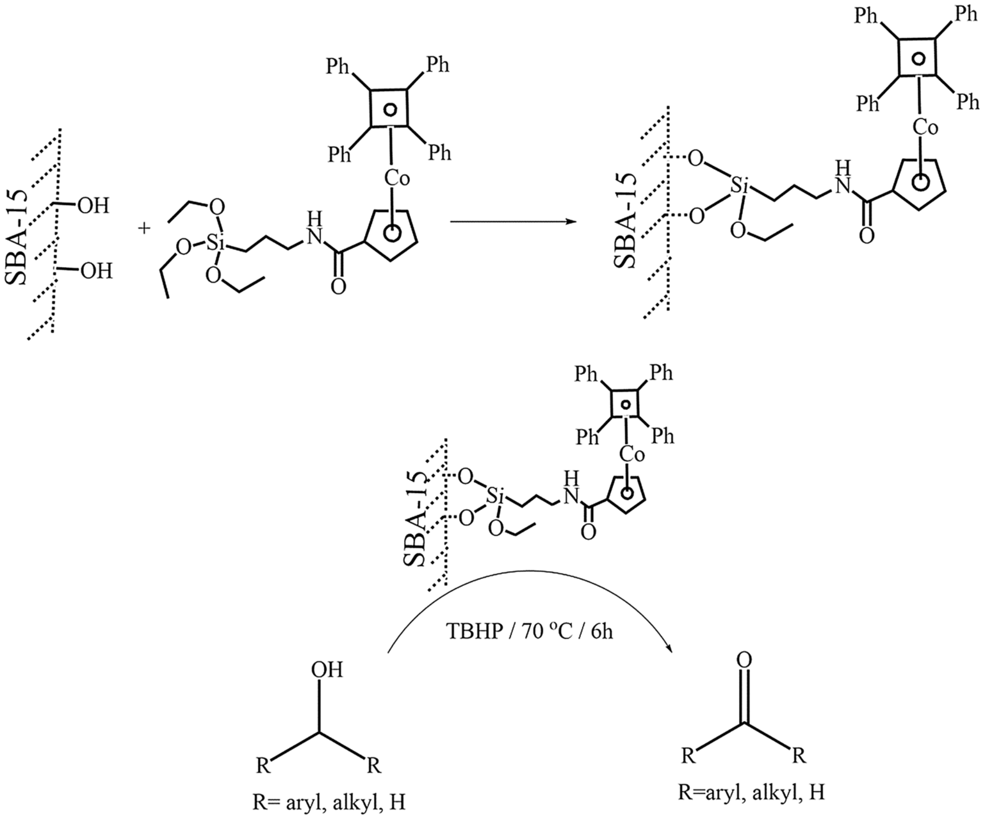

Scheme 2 Schematic representation of complex (**6**) heterogenization on SBA-15 and its application on alcohol oxidation

3 Results and Discussion

Homogenous complex (**6**) was obtained as per the modified procedure described in the literature [34–36] with multi-step route as shown in Scheme 1. The ^{1}H NMR spectrum of synthesized complex showed broad signal around 5.17 ppm which is characteristic of amide functional group along with other signal typical of complex **6** (as shown in Scheme 1). The cobalt content in the complex **6** was calculated by elemental analysis using AAS shows about 7.13 wt%, which is in agreement with theoretical values. Cobalticinium complex containing siloxane functionality was heterogenized on the surface of SBA-15 by refluxing one mmol of complex with one g of support in toluene for overnight. Elemental analyses using atomic adsorption spectrum of the grafted sample revealed the presence of about 0.98 wt% cobalt on SBA-15Co–Si materials. FT-IR spectra of calcined SBA-15 and cobalticinium complex grafted samples (SBA-15Co–Si) are depicted in Fig. 1. Both the samples showed vibrational bands around 1,220, 1,084 and 804 cm^{-1} which is ascribed to stretching frequency of mesoporous Si–O–Si framework vibration [10–15, 33, 34]. SBA-15Co–Si showed additional vibrational band at 1,542 cm^{-1} due to amide (–NH–) functionality derived from cobalticinium complex. In addition, presence of new bands around 2,929, 2,857, 1,498 and 1,451 cm^{-1} respectively can be assigned to the stretching and bending vibrational band of -CH- moiety present in the linker group of complex [10–15, 33, 34]. The powder XRD pattern of calcined SBA-15 and complex **6** grafted samples are shown in Fig. 2. SBA-15 showed three well-resolved peaks around 2θ range of 0.7, 1.4 and 1.7° which is characteristic of (100), (110) and (200) planes of mesoporous hexagonal SBA-15 materials [10–15]. Cobalt complex grafted sample (SBA-15Co–Si) showed the shift in 2θ value in higher angles (2θ in the range of 0.9, 1.6 and 1.8°) corresponds to presence of bulky complex present inside the channel of SBA-15 [14, 15]. Further, it perceives broadening of peaks and decrease in the relative intensities owing to grafting of bulk cobalt complex in the channel of SBA-15 framework. The decrease in interlayer distance from 5.3 to 4.8 nm for SBA-15Co–Si compared to parent SBA-15 again supports the complex **6** located inside the channel of mesoporous molecular sieve.

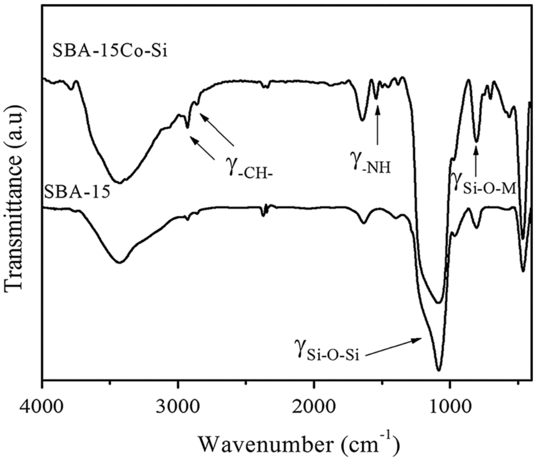

Fig. 1 FT-IR spectra of pure SBA-15 and cobalticinium complex grafted SBA-15 materials

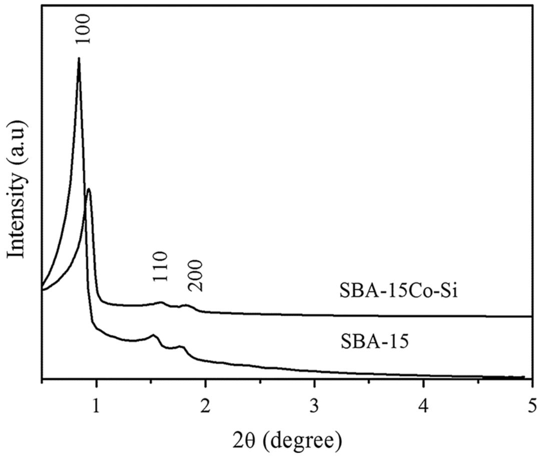

Fig. 2 Powder XRD pattern of SBA-15 and cobalticinium complex grafted SBA-15

Figure 3 depicts the N_2 sorption studies on SBA-15 and SBA-15Co–Si samples. The isotherms are typical of type IV which is based on IUPAC classification and related to mesoporous channels. Compared to SBA-15 material, the SBA-15Co–Si material shows a drastic decrease in pore volume owing to presence of bulk cobalticinium complex (**6**) present inside the channel of SBA-15 mesopores. The textural properties SBA-15 and SBA-15Co–Si are summarized in Table 1. The BET surface area and total pore volume of SBA-15Co–Si material were found to be 388 m^2 g^{-1} and 0.60 cm^3 g^{-1} respectively, which are much lower than the pure SBA-15 material (see Table 1).

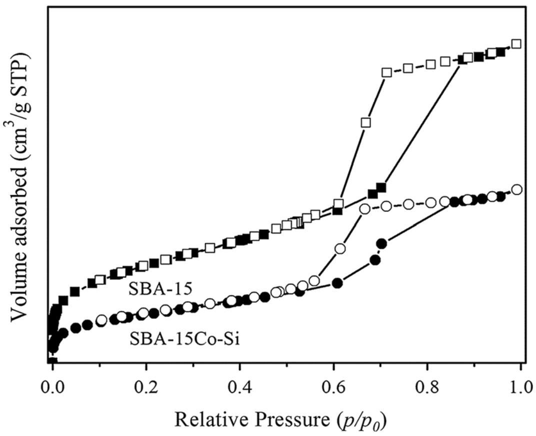

Fig. 3 N_2 sorption isotherms of different SBA-15 materials

Table 1 Textural properties of SBA-15 and SBA-15Co–Si materials

S. no	Sample code	Surface area (m^2 g^{-1})		Pore volume (cm^3 g^{-1})		Average BJH desorption pore diameter (nm)	$D_{(100)}$ (nm)
		BET	Micro pore (t-plot)	Total	Micro pore		
1	SBA-15	769	41.9	1.10	0.018	6.3	5.3
2	SBA-15Co–Si	388	7.80	0.60	0.001	6.0	4.8
3	SBA-15Co–Si[a]	195	–	0.41	0.000	5.2	–

[a] Used catalyst

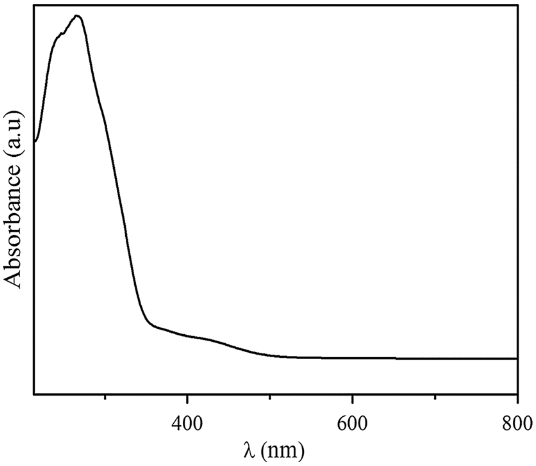

Fig. 4 DR-UV Vis spectrum of cobalticinium complex grafted SBA-15

The decrease in surface area and pore volume confirms that the complex **6** is located on the internal surface of SBA-15 framework. DR-UV–Vis spectrum (Fig. 4) of SBA-15Co–Si shows an intense adsorption band below 250 and 275 nm along with weak band around 415 nm. The absorption band of higher energy in ultraviolet region around 250 nm was assigned to the $\pi \rightarrow \pi^*$ transition which is mainly due to Cp and the other strong band are due to Metal–Ligand charge transfer [37, 38]. The above fact further supports the presence of complex **6** in the channel of mesoporous SBA-15.

The parent SBA-15, and SBA-15Co–Si samples were examined using solid-state ^{29}Si CP-MAS NMR spectroscopy. The parent SBA-15 sample exhibits (Fig. 5) three broad resonances in the ^{29}Si CP-MAS NMR spectrum at chemical shift (δ) values of −110, −101, and −97 ppm, which can be assigned to the Q_4, Q_3, and Q_2 species of the silica framework, respectively [$Q_n = Si(OSi)_n(OH)_{4-n}$].[11–15] The ^{29}Si CP-MAS NMR spectrum of the cobalt complex grafted sample shows a major peak centered around −113 and −106 ppm, attributed to the Q_4 and Q_3 species, and also exhibits additional broad signals between −60.5 and −72 ppm, which can be assigned to the T_2 and T_3 organosilica species, respectively ($T_m = RSi(OSi)_m(OR)_{3-m}$) [10–15], strongly supports that the covalent grafting of complex **6** on the surface of SBA-15 molecular sieves. Further, the ^{13}C CP-MAS spectrum of SBA-15Co–Si (Fig. S2[†]) showed peaks around 7, 27, and 44 which are correspond to different aliphatic functionalities arising from the siloxane functional group [34, 39]. The peak appears around 165 ppm corresponds to the carbonyl functionality, further, the broad peaks present around 72 and 113–123 ppm characteristic of (C_4Ph_4) and phenyl group respectively [34, 39]. The solid state NMR studies reveal that the successful grafting and the structural stability of the complex **6** on the surface of SBA-15 after heterogenization (Fig. 5).

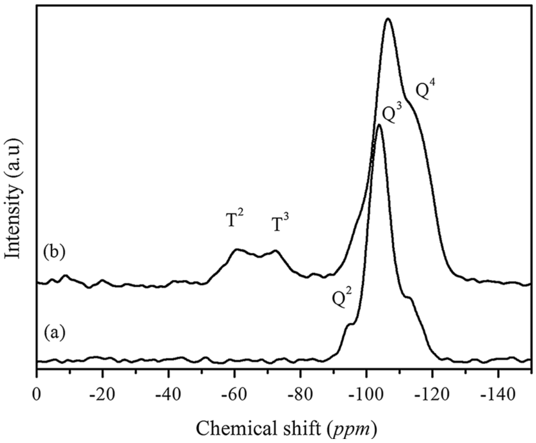

Fig. 5 ^{29}Si CP-MAS NMR spectra of **a** parent SBA-15 and **b** SBA-15Co–Si

Thoroughly characterized SBA-15Co–Si was studied for liquid phase oxidation of benzhydrol in presence of TBHP as oxidant and the results are summarized in Table 2. The SBA-15Co–Si shows about 87 % conversion with nearly 100 % of benzophenone selectivity. Reaction was also studied on pure SBA-15 support and without catalyst, which showed about 18 and 20 % conversion respectively. The above fact supports the presence of cobalticinium complex **6** on the surface of SBA-15 is responsible for the observed catalytic activity. Moreover, the negligible activity observed on filtrate solution further support that there is no leaching of active cobalt species. For comparison, the catalytic activity of homogeneous complex **6** was also studied (catalyst: 100 mg, equivalent to 0.007 mmol of

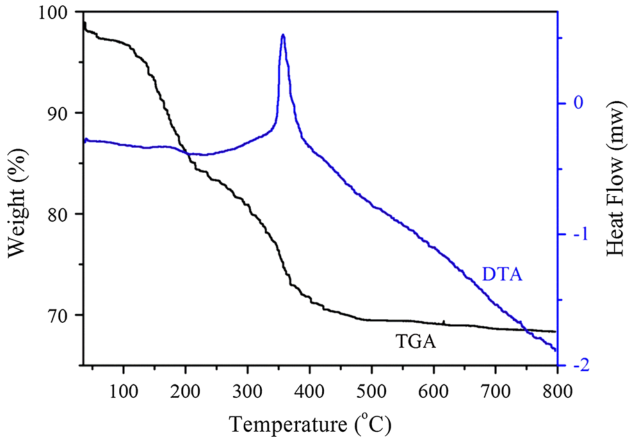

Fig. 6 TGA and DTA profile of used catalyst

Co), which showed about 78 % conversion with TON of 103 which is much less than heterogeneous catalyst. The recyclability of SBA-15Co–Si catalyst was studied after the reaction catalyst washed with dichloromethane (DCM) and it showed comparable activity with the conversion level of 70 % was observed even after two recycles. The observed decrease in catalytic activity is owing to the adsorption of some of organic molecules on the active surface of mesoporous materials [10–15] and it is supported by TG–DTA (Fig. 6). The TG–DTA profile of spent catalyst (Fig. 6) exhibits multiple weight loss, the initial weight loss around 100 °C is due to physisorbed molecules. Drastic change in weight loss around 160–400 °C is due to the decomposition of organic moieties, such as amide functional group and cyclopentadienyl group present on the surface of SBA-15 grafted materials. The accumulation of organic reactant molecule inside the channel of SBA-15Co–Si results in decrease in surface area and pore volume, which is evident from nitrogen sorption analysis (Table 1). Further, the nature of spent catalyst (SBA-15Co–Si-s) was studied by FT-IR analysis (Fig. S3†) and the results are compared with vibrational band of fresh SBA-15Co–Si catalyst. The spent catalyst shows identical vibrational bands as of fresh catalyst (SBA-15Co–Si). However, the intensity of vibrational band corresponds to C–H stretching frequencies (2,860, 2,940 cm^{-1}) on SBA-15Co–Si-s enhanced due to organic reactant molecules adsorbed on the surface. In order to confirm, there is no leaching of cobalt species during the reaction, quenching experiment was carried out by filtering the reaction mixture after 1 h of reaction time and studied for catalytic activity of the filtrate [40, 41]. The filtrate does not show any further conversion, which is strongly supporting that there is no leaching of cobalt complex **6** during the reaction. Furthermore, the filtrate does not have any cobalt species, which is also evident from the AAS analysis. The above fact confirms that the catalysts are truly heterogeneous in nature. SBA-15Co–Si catalyst was further studied for oxidation of various aromatic and aliphatic alcohols and the results are summarized in Table 3. In all the cases, excellent conversions with selective formation of carbonyl compounds were observed and the results are comparable with literature [30]. In addition, cobalt oxide supported on silica and alumina was also studied under identical conditions, which yielded only 23 and 12 % conversion with an exclusive formation of carbonyl compound [23]. Thus, the presence of cobalt complex on the surface of SBA-15 with uniform distribution favors better activity. To understand the mechanistic aspects, the reaction was followed in the presence of radical scavenger BHT (2,6 di-*tert*-butyl-*p*-cresol) and result is shown in Table 2. It is clear from the table that the conversion of alcohol reduced from 87 to 44 % in presence of radical scavenger. The above facts supports that the reaction precedes through radical mechanism on cobalticinim complex grafted SBA-15, which is similar to that of the cobalt based catalyst [23, 42].

Table 2 Oxidation of benzhydrol using various catalysts

S. no	Catalyst	Conversion (%)	TON[c]
1	Without catalyst	18	–
2	SBA-15	20	–
3	Complex **6**	78	103
4	SBA-15Co–Si	87	543
5[a]	SBA-15Co–Si	69	431
6[b]	SBA-15Co–Si	70	437
7[d]	SBA-15Co–Si	44	275

Reaction conditions: Benzhydrol (10 mmol): TBHP (5.5 M in decane) = 1:1, Catalyst = 0.1 gm, T = 70 °C, t = 6 h, Solvent = 5 ml hexane

[a] 1st recycle

[b] 2nd recycle

[c] calculated based on Co-content

[d] Reaction studied in presence of radical scavenger (2 mmol of BHT)

Table 3 Oxidation of various alcohols on SBA-15Co–Si

S. no	Substrate	Catalyst	Product	Conversion (%)	TON
1	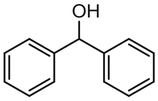	SBA-15Co–Si	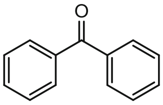	87	543
2	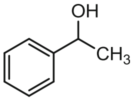	SBA-15Co–Si	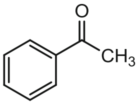	91	568
3	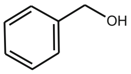	SBA-15Co–Si	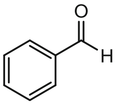	57	356
4	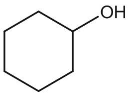	SBA-15 Co–Si	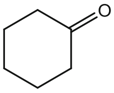	87	543
5	$CH_3–(CH_2)_{10}–CH_2–OH$	SBA-15 Co–Si	$CH_3–(CH_2)_{10}–CHO$	82	512

Reaction conditions: alcohol: TBHP (5.5 M in decane) = 1:1(10 mmol); Catalyst = 0.1 g, T = 70 °C, t = 6 h, Solvent = 5 ml hexane

4 Conclusion

Siloxane functionalized cobalticinium complexes were first time prepared and heterogenized on the surface of SBA-15 molecular sieves. The grafting of complex **6** on SBA-15 was evident from FT-IR, XRD, ^{29}Si CP-MAS NMR and N_2 sorption studies. Heterogenized catalyst showed promising activity for oxidation of benzhydrol and other alcohols into corresponding carbonyl compounds. The catalytic activity remains same after several recycles. There is no leaching of cobalt species from the surface, which is evident from quenching studies.

Acknowledgments The authors are thankful to CSIR (Project No: 01(2516)/11/EMR-II), University of Delhi for their financial support and to USIC, University of Delhi, for the support on instrumentation facility. The authors also wish to express their gratitude for the equipment grant by Humboldt Foundation on FT-IR.

References

1. Simon RA, Mallouk TE, Daube KA, Wrighton MS (1985) Inorg Chem 24:3119
2. Morán M, Cuadrado I, Pineda L, Masaguer JR, Losada J (1990) Inorg Chim Acta 169:119
3. Sisak A (1999) J Organomet Chem 586:48
4. Choualeb A, Rosé J, Braunstein P, Welter R (2003) Organometallics 22:2688
5. Thiel I, Hapke M (2014) J Mol Catal A 383–384:153
6. Sakthivel A, Sathiyendiran M (2014) In: Saji VS, Lopatin SI (eds) Molybdenum and its compounds. Nova Science Publishers, Inc., New York, pp 107–122
7. Kuhn FE, Santos AM, Abrantes M (2006) Chem Rev 106:2455
8. Sakthivel A, Zhao J, Hanzlik M, Kuhn FE (2004) Dalton Trans 3338
9. Zhao J, Sakthivel A, Santos AM, Kuhn FE (2005) Inorg Chim Acta 358:4201
10. Sakthivel A, Zhao J, Hanzlik M, Chiang AST, Herrmann WA, Kuhn FE (2005) Adv Synth Catal 347:473
11. Sakthivel A, Zhao J, Raudaschl-Sieber G, Hanzlik M, Chiang AST, Kuhn FE (2005) Appl Catal A General 281:267
12. Sakthivel A, Zhao J, Kuhn FE (2005) Microporous Mesoporous Mater 86:341
13. Sakthivel A, Zhao J, Kuhn FE (2005) Catal Lett 102:115
14. Sakthivel A, Pedro FM, Chiang AST, Kuhn FE (2007) Dalton Trans 320
15. Sakthivel A, Raudaschl-Sieber G, Kuhn FE (2006) Dalton Trans 468
16. Punniyamurthy T, Velusamy S, Iqbal J (2005) Chem Rev 105:2329
17. Zhan B-Z, Thompson A (2004) Tetrahedron 60:2917
18. Schultz MJ, Sigman MS (2006) Tetrahedron 62:8227
19. Sheldon RA, Arends IWCE, Dijksman A (2000) Catal Today 57:157
20. Brégeault J-M (2003) Dalton Trans 3289
21. Parmeggiani C, Cardona F (2012) Green Chem 14:547
22. Dombray T, Helleu C, Darcel C, Sortais J-B (2013) Adv Synth Catal 355:3358
23. Baskaran T, Kumaravel R, Christopher J, Sakthivel A (2014) RSC Adv 4:11188
24. Baskaran T, Christopher J, Sakthivel A (2014) Adv Porous Mater 2:54
25. Khodakov AY, Chu W, Fongarland P (2007) Chem Rev 107:1692
26. Yang Y, Zhang Y, Hao S, Kan Q (2011) Chem Eng J 171:1356
27. Rana BS, Jain SL, Singh B, Bhaumik A, Sain B, Sinka AK (2010) Dalton Trans 39:7760
28. Centi G, Lanzafame P, Perathoner S (2005) Catal Today 99:161
29. Silva R, Asefa T (2012) Adv Mater 24:1878
30. Rajabi F, Balu AM, Toreinia F, Luque R (2011) Catal Sci Technol 1:1051
31. Badamali SK, Luque R, Clark JH, Breeden SW (2011) Catal Commun 12:993
32. Sheats JE, Rausch MD (1970) J Org Chem 35:3245
33. Rosenblum M, North B, Wells D, Giering WP (1972) J Am Chem Soc 94:1239
34. Singh N, Metla BPR, Elias AJ (2012) J Organomet Chem 717:99
35. Wang L, Reis A, Seifert A, Philippi T, Ernst S, Jiab M, Thiel WR (2009) Dalton Trans 3315
36. dos Reis EF, Campos FS, Lage AP, Leite RC, Heneine LG, Vasconcelos WL, Portela Lobato ZI, Mansu HS (2006) Mater Res 9:185

37. Giordano PJ, Wrighton MS (1977) Inorg Chem 16:160
38. Hou XF, Pang Z, Xu Y-F, Cai R-F, Huang Z-E (2000) Chinese J Chem 18:733
39. McKittrick MW, Jones CW (2003) Chem Mater 15:1132
40. Lempers HEB, Sheldon RA (1998) J Catal 175:62
41. Sakthivel A, Selvam P (2002) J Catal 211:134
42. Arends IWCE, Sheldon RA (2001) Appl Catal A 212:175